# CHAPTER - VIII

# CHAPTER-VIII

# ION IRRADIATION INDUCED INTER- AND INTRA-GRANULAR MODIFICATIONS IN $YBa_2Cu_3O_7$ AND $YBa_2Cu_3O_7$/Ag COMPOSITE THICK FILMS

## VIII.1 Introduction

The present chapter reports the response of granular sintered cuprates to swift heavy ion (SHI) irradiation. Two ion beams, one, 120 MeV S and the other, 250 MeV Ag ion beams have been used in the present study. These ion beams are choosen such that the lower energy lighter ions can only create atomic size point defects and the higher energy heavier ions create amorphized latent tracks in the grains of $YBa_2Cu_3O_{7-y}$ (YBCO). The sintered YBCO system consisting of randamomly oriented highly anisotropic grains separated by grain boundaries however presents a complex system to SHI irradiation[1] effects because of the conducting nature of the former and insulating nature of the latter. We analyze the evolution of the temperature dependent resistivity characteristics of YBCO and YBCO/Ag composite thick films with irradiation fluence and probe into the inter and intragranular modifications induced by these ions.

## VIII.2 Experimental

Thick films of YBCO were prepared on $Y_2BaCuO_5$ insulating substrate by diffusion reaction technique as detailed in chapter-III. The films were irradiated with 120 MeV S and 250 MeV Ag ions using the 16 MV tandem pelletron accelerator at NSC, New Delhi. To study the effect of granularity in controlling the irradiation response of YBCO, different batches of films with

same chemical composition but with varying normal state electrical resistivities (ρ) were prepared. The differences in ρ are associated with differences in grain structure, grain dimensions, grain orientation and intergrain contacts of the films which were controlled by controlling the sintering schedule and by having Ag in the intergrain boundaries.

In-situ resistance measurement as a function of temperature was done after irradiating the samples with an ion beam at different fluence levels. After each cycle of irradiation and resistivity data acquisition as a function of temperature, the target was cooled to 79 K before the next cycle of irradiation and data acquisition began. The details of the resistivity setup and sample cooling arrangement is given in chapter III.

## VIII.3 Results and Discussion

Table VIII.1 gives the TRIM-95 calculation of the electronic energy loss, $S_e$, the nuclear energy loss, $S_n$ and the range, $R_m$ of the two ion beams in YBCO. A comparison of the magnitudes of $S_e$ and $S_n$ indicates that the dominant energy loss mechanism for both the ion beams is through inelastic interaction of the ions with the target electrons ($S_e$). The $S_n$ induced effects which ordinarily dominates at the end of the trajectory of swift heavy ions is suppressed in the present situation since the thickness of the films (~10 μm) is less than the range of the ion beam. The modifications brought about by the ion beams in the YBCO films is therefore primarily due to the $S_e$ induced effects. In a homogeneous medium, these modification include annealing of defects [1], additional defects [2], resistivity enhancement [3], phase change [4-6], creeping in amorphous materials [7] and tracks in metallic crystalline alloys [8] and in insulating oxides [9,10]. The granular cuprates with conducting grains separated by insulating grain boundaries however present an inhomogeneous medium. The response of these systems therefore is expected to be different from that of the homogeneous medium considered above. In addition to some of these effects of ion irradiation observed in

homogeneous medium, additional effects like disintegration of grains [11] and grain alignment [12] are expected in granular cuprates due to confinement of irradiation induced thermal spike in small size grains and random orientation of highly anisotropic grains respectively. Further, the cuprates are a class of materials which exhibit a positive temperature coefficient of resistivity like that in metals. Their conductivity however is many orders of magnitude lower than classical metals. Since SHI induced modifications in a material largely depends on its electrical conductivity, the response of the cuprates to SHI irradiation falls apart from that in metals and insulators.

**TABLE. VIII.1** TRIM-95 calculation of the electronic energy loss ($S_e$), nuclear energy loss ($S_n$) and the range ($R_m$) of 120 MeV S and 250 MeV Ag in YBCO.

| Ion Beam | $S_e$ (keV/A) | $S_n$ (eV/A) | $R_m$ (μm) |
|---|---|---|---|
| 120 MeV S | 0.3792 | 3.041 | 29 |
| 250 MeV Ag | 2.0 | 5.7 | 15 |

The threshold electronic energy loss ($S_{eth}$) of a SHI to create amorphized latent tracks in YBCO has been found to be 1.44 keV/A [13]. The ion with $S_e$ greater than this threshold and less than this threshold are therefore expected to have widely different effects in this system. These effects have been studied to a great extent in epitaxial thin films and single crystals of the cuprates [14]. In granular cuprates, these studies are rather rare. This is largely due to the fact that these systems present a heterogeneous medium to SHI where the modifications of both the grains and grain boundaries are involved and the interpretation of the results became difficult. Based on a percolation current conduction model as discussed in chapter VI,

we have therefore confined ourselves to extract the granularity parameters from the temperature dependence of resistivity data in a set of YBCO thick films and studied their evolution with irradiation fluence. We first discuss 120 MeV S ion irradiation induced modifications in YBCO where the $S_e$ is less than the threshold to create amorphized latent tracks. The effect of 250 MeV Ag ion irradiation where $S_e$ is greater than this threshold is discussed later.

### *VIII.3.1 120 MeV S ion irradiation effect*

The temperature dependent resistivity characteristics of YBCO thick films irradiated with 120 MeV S-ions at various fluences is shown in Fig. VIII.1. In agreement with observations made by many [15-18], we observed the decrease of Tc and increase of normal state resistivity with increasing irradiation fluence. As seen from Fig. VIII.2 the $Tc_0$ where superconducting percolation is established through weak link networks, decreased faster than Tc where grains start superconducting. At higher fluences, $Tc_0$ went below 79 K and its fluence dependence could not be followed. Following the fluence dependence of Tc (Fig. VIII.3), it can clearly be seen that Tc decreases by about 1.5 K with the maximum dose of irradiation which was $2.334 \times 10^{13}$ ion/cm$^2$. The negligible change in Tc even at this high fluence indicates that not much permanent defects are created due to 120 MeV S-ion irradiation. Following the variation of Tc with irradiation fluence, it can be seen that Tc shows a sharp decrease at the first dose of irradiation beyond which it decreases slowly. This sharp decrease in Tc at the first dose of irradiation as will be discussed in section VIII.3.2.5 is a consequence of frozen in point defects induced by irradiation at low temperature (79 K)

To study the irradiation effect on inter and intragrain resistivity of the thick film, we analyzed the normal state resistivity and its temperature dependence based on the percolative conduction model as detailed in chapter VI. The parameters $\rho_{wl}$ and $\alpha$ which quantify granularity are thus evaluated.

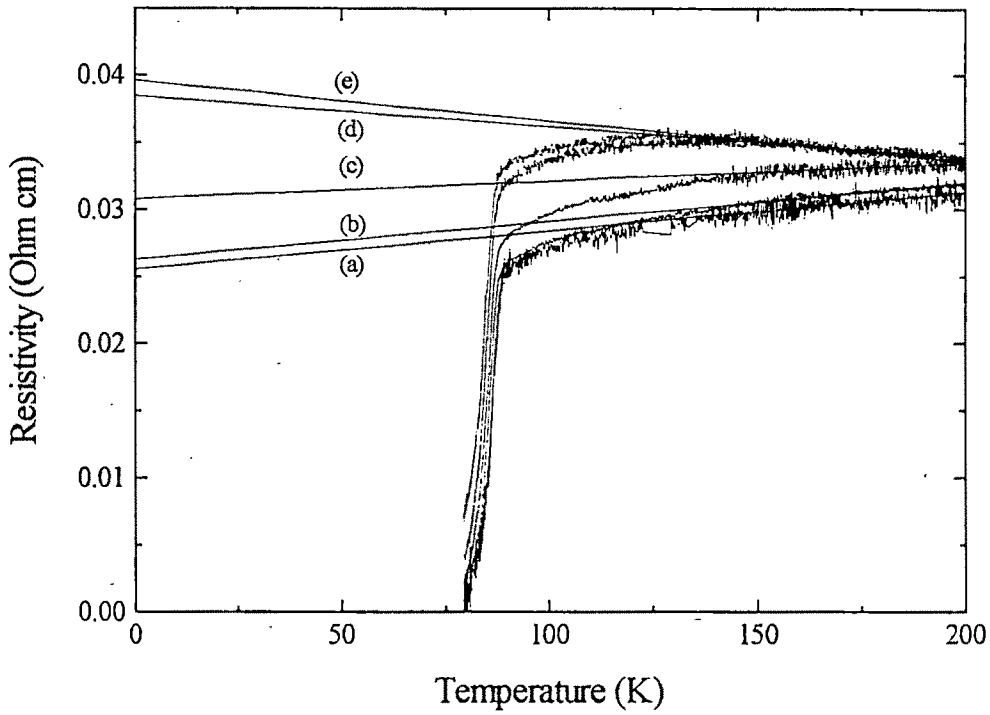


Fig.VIII.1. The evolution of temperature dependence of the resistivity characteristics of $YBa_2Cu_3O_{7-y}$ thick film irradiated with 120 MeV S-ion at different fluences. (a) Unirradiated (b) $3.91x10^{10}$ ions/cm$^2$ (c) $3.91X10^{12}$ ions/cm$^2$ (d) $1.172X10^{13}$ ions/cm$^2$ (e) $2.344X10^{13}$ ions/cm$^2$.

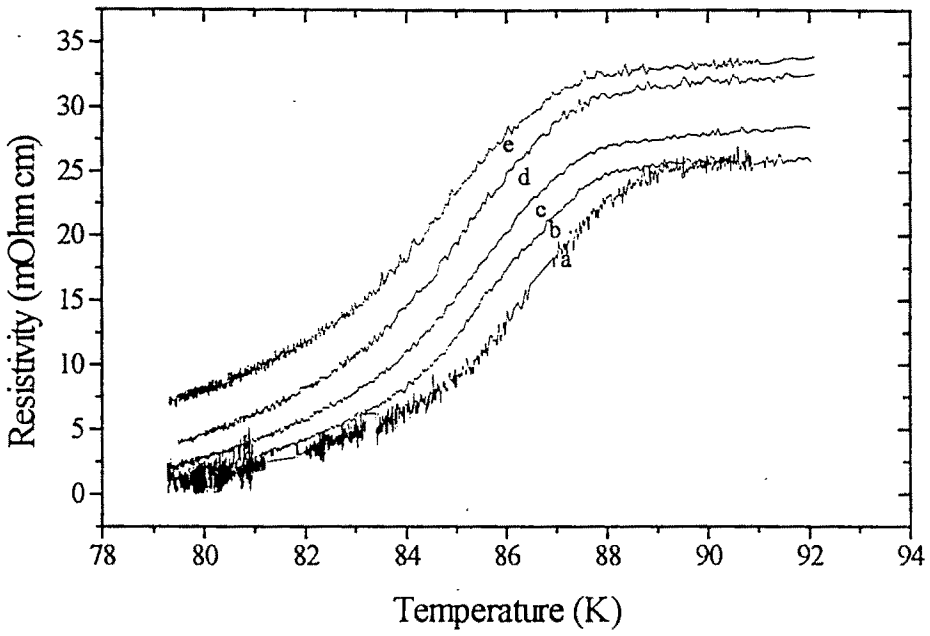


Fig.VIII.2. The ρ vs T characteristics of the $YBa_2Cu_3O_{7-y}$ thick films taken close to the superconducting transition region after irradiation with 120 MeV S ions at different fluences. The figure indicates a faster decrease of $Tc_0$ than Tc. (a) Unirradiated (b) $3.91x10^{10}$ ions/cm$^2$ (c) $3.91X10^{12}$ ions/cm$^2$ (d) $1.172X10^{13}$ ions/cm$^2$ (e) $2.344X10^{13}$ ions/cm$^2$

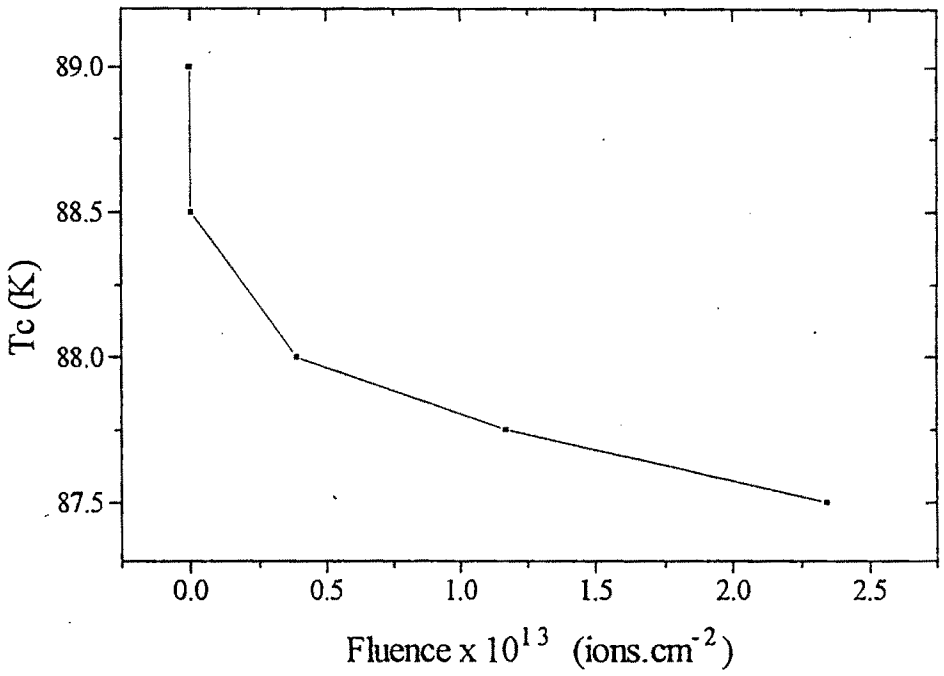


Fig.VIII.3. Fluence dependence of Tc of $YBa_2Cu_3O_{7-y}$ thick film irradiated with 120 MeV S-ion.

The variation of these parameters along with the variation of $d\rho/dT$ and $\rho_0$ at different fluences is given in Table VIII.2.

**TABLE VIII.2.** Variation of the parameters, quantifying granularity in YBCO sample irradiated with 120 MeV S-ion

| fluence ions/cm$^2$ | $\rho_{100k}$ (m ohm cm) | $d\rho/dT$ ($\mu$ ohm cm $K^{-1}$) | $\rho_0$ (m ohm cm) | $\rho_{wl}$ ($\mu$ ohm cm) | $1/\alpha$ | Tc (K) |
|---|---|---|---|---|---|---|
| 0 | 27.06 | 28.64 | 25.56 | 446.2 | 57.14 | 89.0 |
| $3.91x10^{10}$ | 27.54 | 28.46 | 26.29 | 462.0 | 56.82 | 88.5 |
| $3.91X10^{12}$ | 29.63 | 13.18 | 30.81 | 1168.4 | 26.39 | 88.0 |
| $1.172X10^{13}$ | 33.71 | - | - | - | - | 87.75 |
| $2.344X10^{13}$ | 34.58 | - | - | - | - | 87.5 |

Since current percolation influences both $\rho_0$ and $d\rho/dT$ to the same extent (eqns. VI.5 and VI.6), it is expected that these parameters should show similar trend of variation with variation in the sample quality due to ion irradiation. In fact, Halbritter et al.'s [19]observation of $d\rho/dT$ scaling with $\rho_0$ in a set of granular YBCO samples and thus showing an apparent deviation from the Mattheissen's rule, led them to propose the percolative current conduction model in heterogeneous systems [19]. Scaling of $d\rho/dT$ with $\rho_0$ has also been observed by others [20] and is also seen in the case of our YBCO/Ag composite bulk and thick film samples with varying Ag content

(chapters-VI and VII). Table VIII.2 however, shows that though $\rho_0$ increases with increasing fluence, $d\rho/dT$ shows a decrease.

This is in clear contrast to generally observed correlation in the variation of $\rho_0$ and $d\rho/dT$ with the quality of the granular cuprate superconductors. This observation therefore points to a very different kind of modifications that SHI irradiation induces in granular YBCO thick films as compared to the effect of varying the sintering condition or even varying the Ag content to modify granularity. To gain an understanding of the SHI induced modifications in the granularity of our films, we analyze the evolution of the parameters $\alpha$ and $\rho_{wl}$ which contribute to evolution of $d\rho/dT$ and $\rho_0$ as shown in eqns. VI.5 and VI.6.

Since irradiation induced defect scattering of charge carriers is temperature independent, the temperature coefficient of the intragranular resistivity $d\rho_{ab}/dT$ is not expected to show fluence dependence. The opposite trend in the variation of $d\rho/dT$ and $\rho_0$ with ion fluence is therefore expected to arise due to the opposite trend in the variation of $1/\alpha$ and $\rho_{wl}$ with fluence. These latter two parameters evaluated from the $\rho$ vs T characteristics as outlined above and as shown in Table VIII.2 do in fact show the opposite trend in variation with fluence. While $\rho_{wl}$ increases with fluence, the $1/\alpha$ shows a decrease at higher fluence, the implication of which is discussed below.

### *VIII.3.1.1. Irradiation destroys cou pling across grain boundaries*

The magnitude of $\rho_{wl}$ represents the average weak link resistivity in a granular medium [21]. The tail in the low temperature region of superconducting transition is infact a consequence of the distribution of $\rho_{wl}$'s of individual weak links. With increase of fluence, $\rho_{wl}$ increases from 446.2 μohm cm for unirradiated to 1168.4 μohm cm for irradiated sample with fluence of $3.9 \times 10^{12}$ ions $cm^{-2}$ (Table VIII.2). At still higher fluence, the $\rho$ vs T

shows semiconducting nature. This implies that the grain boundaries are the ones which are affected the most during ion irradiation. At higher fluences, the grain boundaries become insulting and the grain boundary thickness increases. Similar observations have also been made under irradiation of granular films with ions in the GeV range where it was assumed that irradiation affects the grain boundaries faster than the grains and suppresses tunneling of charge carriers across the grain boundaries [22].

### *VIII.3.1.2. Irradiation induced grain alignment*

The percolation factor $\alpha$ has the contribution of both the misalignment factor f and structural factor $\alpha_{str}$. The decrease of the factor $1/\alpha$ with irradiation fluence indicates that current frustration in the irradiated sample is less as compared to that in the unirradiated ones. This interesting aspect of irradiation in inducing improvement in the sample quality with improved current percolation is a consequence of modifications of the two constituent parameters of $\alpha$. i.e. f and $\alpha_{str}$ due to irradiation. The factor $\alpha_{str}$ accounting for the current frustration due to pores, voids and micro cracks is not expected to be much influenced by irradiation. Therefore, the influence of irradiation on $\alpha$ is solely due to the irradiation induced modification of the grain alignment factor f.

Our result of $1/\alpha$ decreasing with irradiation fluence thus indicates that irradiation induces grain alignment in a system of randomly oriented anisotropic non-spherical grains. While the mechanism of irradiation induced grain alignment in YBCO system is still not clear, it is speculated that in YBCO thick films with randomly oriented grains, the grains whose one of the major axis is parallel to the direction of the projectile ions, channel these ions. As a result, these grains are not affected much by irradiation. Other grains whose axis do not coincide with the direction of the ion beam, do not channel the ions. These grains receive the maximum energy of the beam. These grains therefore disintegrate and regrow along the direction of the ion beam. Such a

situation can lead to irradiation induced grain alignment in YBCO system as observed in the present case.

### *VIII.3.2 250 MeV Ag ion irradiation effect*

The electronic energy loss $S_e$ of 250 MeV Ag ions in YBCO is larger than the threshold energy loss ($S_{eth}$) to create amorphized latent tracks in this system (Table VIII.1). A large number of studies have dealt with the effective use of these tracks for flux pinning and Jc enhancement in the superconducting state of YBCO [23]. Most of these studies have used either single crystals or epitaxial thin films where the contribution of grain boundaries to the transport properties is negligible. The response of these systems to SHI irradiation is largely governed by the modifications induced into their grains. Only a few studies exist in the literature which deal with the SHI induced modifications in YBCO films having a relatively high concentration of grain boundaries [24]. In these systems, the grain boundaries having higher resistivities and higher disorder get damaged faster than the grains under SHI irradiation.

The sintered thick films used in the present study were prepared by diffusion reaction technique. Because of the very preparation procedure, the contribution of grain boundaries to the transport properties of our films cannot be neglected. In an earlier study [25] we have shown that sintered thick films of YBCO are highly sensitive to SHI irradiation and the prominent defects created during irradiation are mostly due to the grain boundaries getting degraded faster than the grains (VIII.3.1.1).

The two extrinsic factors which influence current transport in the granular medium of the sintered YBCO films are the weak link resistivity $\rho_{wl}$ across the grain boundaries and the current percolation factor $1/\alpha$ due to the grain misalignment, and voids and microcracks. The irradiation response of the thick films is therefore a consequence of the irradiation induced modifications of these two parameters. Evolution of granularity in the films

with irradiation fluence are quantified by these two parameters. These parameters as discussed earlier were estimated from the ρ vs T characteristics (Fig. VIII.4). Table VIII.3 gives the variation of these parameters with irradiation fluence. Like in the case of 120 MeV S-ion irradiation, 250 MeV Ag ion irradiation also induces grain decoupling and grain alignment as evidenced from the increase in $\rho_{wl}$ and decrease in $1/\alpha$ respectively.

Our earlier studies [12] on SHI induced modifications in YBCO/Ag composite thin films have revealed the irradiation insensitivity of these films due to Ag occupying grain boundaries and inducing microstructural modification in these films. In bulk and thick films of YBCO/Ag composites, we have also shown that Ag suppresses grain boundary resistivity and brings about grain alignment [26] (chapter VI and VII). Goto et al. [27] and Kumar et al. [28] have shown that the composite transport characteristics are the best when Ag content in the composites is 10 wt.%. The 250 MeV Ag irradiation effect was therefore confined to YBCO/Ag composites with 10 wt.% Ag.

*VIII.3.2.1. Tc variation with irradiation fluence*

Fig. VIII.4 shows the evolution of temperature dependence of the resistivity characteristics of YBCO thick films irradiated with 250 MeV Ag-ions at various fluences. Unlike in the case of 120 MeV S ion irradiation, which results in a monotonic decrease of Tc with increasing fluence, the 250 MeV Ag ion irradiation of YBCO leads to an unusual variation of Tc with fluence. At the first dose ($5x10^{10}$ ion $cm^{-2}$) of Ag ion irradiation, the Tc dropped suddenly from 91.5 K to 82.5 K (Fig. VIII.5). This rapid rate of Tc decrease was seen to be arrested at higher fluences. The Tc in fact showed an increasing trend beyond the initial fluence and attained a value of ~ 86 K at the maximum fluence used in the present study i.e. $5 \times 10^{11}$ ion $cm^{-2}$. At still higher fluence the Tc is expected to show the usual trend of decrease as observed by others [15-17].

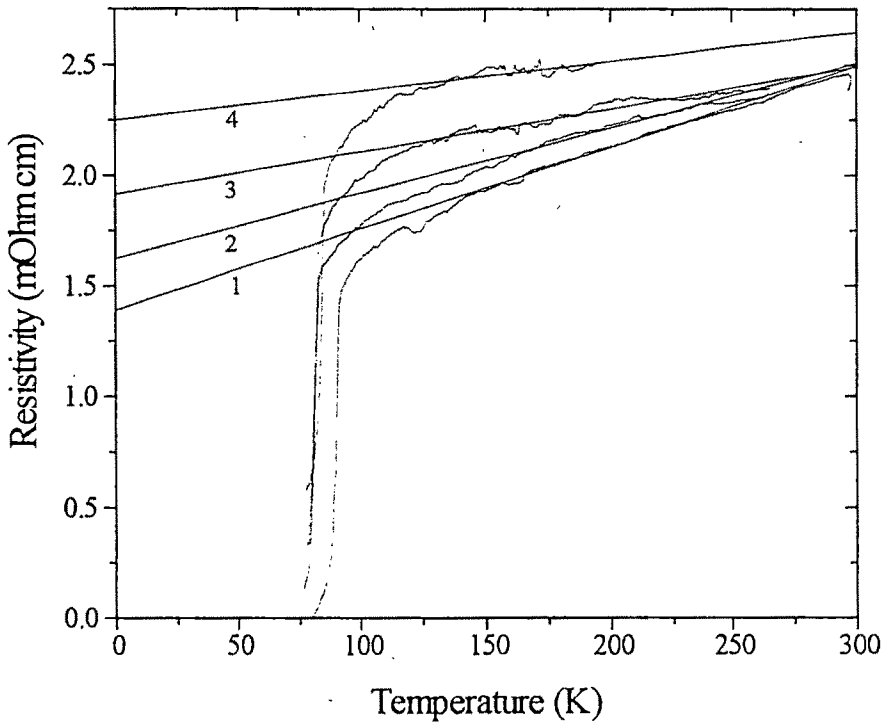


Fig.VIII.4. The evolution of temperature dependence of the resistivity characteristics of YBCO/Ag (10 wt.%) composite thick film irradiated with 250 MeV Ag-ions at various fluences (1) Unirradiated (2) $5x10^{10}$ ions/cm$^2$ (3) $1x10^{11}$ ions/cm$^2$ (4) $5x10^{11}$ ions/cm$^2$.

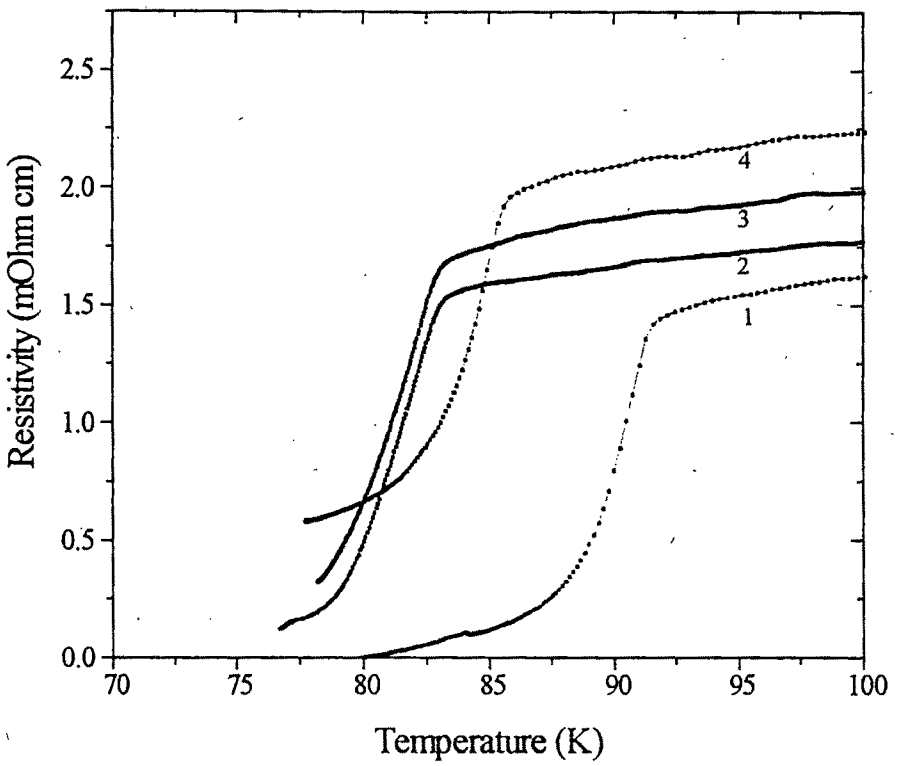


Fig.VIII.5. The ρ vs T characteristics of the YBCO/Ag (10 wt.%) composite thick film taken close to the superconducting transition region after irradiation with 250 MeV Ag ions at different fluences. (1) Unirradiated (2) $5x10^{10}$ ions/cm$^2$ (3) $1x10^{11}$ ions/cm$^2$ (4) $5x10^{11}$ ions/cm$^2$. At the first dose of irradiation, Tc dropped suddenly from 91.5 K to 82.5 K (2) and then slowly increased at higher fluences (3 and 4).

**TABLE VIII.3** Variation of the parameters, quantifying granularity in YBCO/Ag10wt.% sample irradiated with 250 MeV Ag-ion.

| Fluence ions/cm$^2$ | $\rho_{100K}$ (m ohm cm) | $d\rho/dT$ ($\mu$ ohm cm K$^{-1}$) | $\rho_0$ (m ohm cm) | $\rho_{wl}$ ($\mu$ ohm cm) | $1/\alpha$ | Tc (K) |
|---|---|---|---|---|---|---|
| 0 | 1.62 | 3.68 | 1.39 | 189.25 | 7.35 | 91.5 |
| $5x10^{10}$ | 1.77 | 2.95 | 1.62 | 275.55 | 5.88 | 82.5 |
| $1x10^{11}$ | 1.98 | 1.93 | 1.91 | 496.88 | 3.85 | 83.5 |
| $5x10^{11}$ | 2.24 | 1.32 | 2.25 | 849.38 | 2.66 | 86 |

The decrease of Tc with increasing fluence is an expected effect of irradiation with high energy heavy ions which damages the weak link coupling at the grain boundaries and destroys the superconducting phase coherence. Not just the grain boundaries, the grains themselves get damaged when the $S_e > S_{eth}$. From TRIM 95 calculation, the $S_e$ of 250 MeV Ag beam in YBCO is ~ 2 keV/A. This $S_e$ being greater than the $S_{eth}$ (1.44 keV), columnar tracks are produced in the YBCO due to irradiation. The latent track formation in this range of Se of SHI irradiation in YBCO has been observed by many workers [29,30]. The track radius r is reported to be ~ 5 nm [31]. For a fluence of 5 $x10^{10}$ ions/cm$^2$, the damage area is calculated to be 5 x $10^{-2}$ cm$^2$. With such a low fraction of the damage area, the percolative conduction path in the composite sample cannot be eliminated. So Tc degradation for the initial fluence is not expected from the tracks. But Tc is observed to decrease by ~ 10 K (Table VIII.3) for the initial fluence of 5 $x10^{10}$ ions/cm$^2$. To understand this unexpected decrease of Tc in the low fluence regime of 250 MeV Ag ion irradiation of YBCO, we analyze the possible mechanisms of ion matter interaction and 250 MeV Ag ion induced track creation.

*VIII.3.2.2. Ion-matter interaction*

A large number of studies [6] have indicated that the phenomenon of SHI induced track registration is material dependent. It appears that neither ion-explosion model nor the thermal spike model is satisfactory in explaining the irradiation induced modifications in materials [32]. The concept of "coulomb explosion" i.e. violent disruption of a local region of the lattice by unbalanced electrostatic forces during the period before electrical neutrality is restored to a region around the ion track, has its applicability strongly dependent on electron mobility in materials. The track creation in insulating materials is thus successfully explained by this model. In later years, SHI induced tracks have also been observed in certain metals [8,33] and semi-metals [8]. In the thermal spike model [34], the time needed for energy transfer from an incident ion to the excited electron gas is much less than the typical time scales of lattice vibration. Thus, the energy loss from the incident ion can be regarded as instantly transferred to the gas of excited electrons. Then the energy of electronic excitations is very quickly converted into thermal energy of the lattice in a very localized region. The rapidity with which the energy is transferred from the hot electrons to the lattice of ions depends on whether the material is metallic, semiconducting or ionic in increasing order of rapidity [6]. Arguments in favour of and against the applicability of both the models in various systems have been given in the literature [32,35]. Modifications of these models to extend their applicability to specific systems have also been attempted [30]. To explain the unexpected Tc suppression in the low fluence regime of irradiation, we consider below a model proposed by Izui [36] and named as time dependent line source model. In particular, we analyze the role of secondary electrons produced during irradiation in creating atomic size point defects in addition to the amorphized latent tracks produced by the ions themselves.

*VIII.3.2.3. SHI irradiation induced secondary electron emission*

Electron emission is one of the most conspicuous consequences of inelastic ion-surface collisions and, in general, of interactions of any ionizing radiation with condensed matter. Using electron spectroscopic techniques, Zaefel et al. [37] have observed pronounced electron emission jets around the projectile direction for a wide range of projectile beams from protons to Au with energies ranging from 0.2 to 3 MeV/u. Time dependent line source model considers energy distribution of secondary electrons excited by an ion, various collision processes of these electrons and relaxation time in energy transfer from electrons to lattice. The basic idea of this model is as follows: Secondary electrons are produced with energies ranging from a few eV to 1 keV in narrow range cylindrical region of about 1 nm in diameter along the path of an ion. Among these excited electrons, electrons with relatively high energy quickly escape from this region leaving a row of positively charged clouds. On the other hand electrons with relatively lower energies are bound in this narrow region by coulomb attraction of these positive atoms. A line of extremely high energetic charge cloud along the ion path is thus created. The consequence of this line source can be two fold. The positively charged atoms in the cylindrical zone around the line created due to the escape of high energetic electrons forms a space charge which can explode by the process of coulomb explosion [13,31,38] due to unbalanced electrostatic forces. As a result, columnar defects are produced by the resulting cylindrical shock waves. On the other hand, the relatively low energetic electrons bound in the narrow cylindrical region can transfer their energies to the lattice by electron-phonon interaction [30]. If the consequent temperature rise exceeds the melting temperature of the lattice, the lattice in the narrow cylindrical zone melts and quenches with an extremely high quenching rate ~ $10^{13}$ to $10^{14}$ K/s. An amorphous latent track is thus formed around the ion path.

Whatever may be the mechanism for the formation of SHI induced amorphized columnar tracks, their number at an ion fluence of $5x10^{10}$ ions/cm$^2$ is much less to account for the observed Tc reduction. We therefore

consider the effect of high energetic secondary electrons which escape out of the track region in the process of materials modification. These secondary electrons emitted radially around the ion track can have a much larger interaction cross section around the ion path than the tracks created by the ions themselves. However, unlike the high energetic ions which create amorphized latent tracks, the electrons can, in principle induce only point defects.

*VIII.3.2.4. Defect creation due to secondary electron irradiation*

Electron irradiation has been proved to be one of the best ways of creating uniformly distributed point defects in solids [34]. The energy required to displace Y, Ba, Cu, and O atoms in YBCO structure has been found to be 532, 730, 413 and 129 keV respectively. Because of the low activation energies involved for oxygen mobility, point defects due to electron irradiation are created mostly at the oxygen sites. This process leaves the overall oxygen content unchanged and atoms are displaced into interstitial positions.

Because of the complex crystal chemistry of the cuprates, there has been a lot of controversy on the threshold energy for the creation of oxygen defects. The fixed five fold oxygen coordination of Cu(2) ions make the plane and apical oxygen ions strongly bound to the Cu ions. The threshold value of energy for the displacement of these ions is therefore quite high (~130 keV). The chain oxygens however are loosly bound and can have a lower displacement energy. Tolpygo et al. [39] for example observed this threshold value to be 58 keV. In oxygen deficient samples, the threshold energy was found to be even lower. Defects at the chain site could thus be produced with lower energy (20- 40 keV) electron irradiation [39]. The displacement energy, $E_d$ per ion for plane and chain oxygens was evaluated to be 8.4 and 2.8 eV respectively. Using a molecular dynamics simulation of oxygen displacements from O(1) to O(5) sites, some authors [39,40] have found displacement energy to be as low as 1.5 eV which is close to oxygen diffusion

activation energy 1.3 eV. The energy barrier between the chain site and interstitial position on the a-axis is low and chain disordering can be induced by nonequilibrium phonons which are the final product of energy release after any collision event. Thus, the secondary electrons radially emitted from the track of each ion can in fact induce point defects in a structure like the YBCO.

Though the diameter of the amorphized latent tracks created by 250 MeV Ag ions in YBCO may be 5 to 10 nms [30], the diameter of the cylindrical zone around the ion tracks where point defects are created due to secondary electrons is expected to be much larger, even approaching the range of the electrons in the YBCO medium. For 10 keV electrons, this range can be 1μm [39]. Further, the number of secondary electrons coming out of a track due to a single ion impact is expected to be quite large. Thus, each electron creating a large number of point defects and each ion creating a large number of such electrons can lead to the formation of a much larger number of point defects spread over a large area around the ion path which can account for the observed Tc suppression even for low fluence ~ $5x10^{10}$ ions/$cm^2$.

### *VIII.3.2.5. Tc suppression due to electron irradiation induced point defects*

Suppression of Tc in YBCO type superconductors due to electron and light ion irradiation has been reported by many [41]. In all these cases, the Tc suppression is largely due to the point defects created during irradiation. There are basically two ways through which the point defects can suppress Tc depending upon their location. If the point defects are located in the superconducting $CuO_2$ planes, they can cause pair breaking due to potential impurity scattering [42,43]. In the chains, the point defects can influence the carrier concentration and hence suppress Tc. The displacement of oxygen atoms from b-axis (chains) to the originally vacant sites along the a-axis due to electron irradiation for example transforms the square-planar coordination

of the chain-site Cu atoms into a non-square planar four-fold coordination [40]. This coordination geometry drastically reduces the hole-carrier density in the $CuO_2$ plane (charge conduction plane) and leads to Tc suppression. Considering the relatively less energy required for the creation of defects on the chain oxygen site, we suggest that the secondary electrons, emanating from the high energy ion tracks, disorder the chain oxygens and reduce Tc of the films.

From the above discussion, it seems that during 250 MeV Ag ion irradiation of YBCO thick films, point defects due to secondary electrons are created along with the amorphized latent tracks created by the ions themselves. It may be emphasized here that the irradiation was performed at 79 K and the resistance vs temperature data was acquired during heating of the sample to room temperature. After the first dose of irradiation, the point defects created due to secondary electrons were frozen in and the observed Tc decrease from 91.5 K to 82.5 K is a consequence of these point defects. During data acquisition, the temperature was slowly raised to 300 K and most of the point defects get annealed out during the temperature rise. The annealing of point defects at higher temperatures is evident from the resistivity plot of the irradiated samples which tend to converge with that of the unirradiated sample with increasing temperature. Annealing of point defects in YBCO at high temperature has also been seen by others. Albenque et al. [22] have reported that 60 % of the irradiation induced damages can be recovered after annealing the sample to 280 K. Other reports [44] show that above 150 K, the thermally activated defects anneal out in YBCO sample. We therefore presume that the point defects created during irradiation at 79 K freeze at this temperature. The Tc being close to 79 K, it is affected by these frozen point defects. The point defects however get annealed out at higher temperature. A more systematic study with data acquisition during cooling cycle also would have shown a hysteresis effect in the temperature vs resistivity characteristics with Tc approaching to that of the unirradiated sample and would have clearly established this annealing effect. This

experiment however could not be done due to difficulty in controlling the temperature of the sample inside the irradiation chamber during the cooling cycle. After the initial Tc degradation arising due to the first dose of irradiation, the Tc did not decrease further on subsequent irradiation cycles upto a fluence of $5x10^{11}$ ions/cm$^2$ (Fig. VIII.6). In fact, a slight increase of Tc was observed in this fluence range. This observation in a way proves that point defects created due to irradiation at 79 K are frozen in and cause degradation of Tc by 9 K from the initial value of 91.5 K. The restoration of Tc due to annealing of these defects however was not observed..

In accordance with the observation on Tc variation with irradiation fluence in single crystals and epitaxial thin films [24], the Tc of our samples should have shown a monotonic decrease with increasing fluence. The almost fluence independence or even a slight increase of Tc beyond the initial fluence of 5 $x10^{10}$ ions/cm$^2$ in our samples is therefore associated with their inherent granularity. The grain boundaries and oxygen deficient regions in the grains are known to act as weak links to superconduction in sintered YBCO samples. Sudarsan et al. [14] have observed that displacement of oxygen from the columnar tracks to the oxygen deficient regions of Bi-system irradiated with 107 MeV Ag ion eliminates weak links by irradiation. Further, Ag residing at the grain boundaries in the composite films has a strong affinity for oxygen [28]. Thus, the oxygen ions which are liberated from the ion tracks during irradiation can migrate over a much larger distance compared to the ion track radius and provide a healing effect in the oxygen deficient regions and grain boundaries. The SHI irradiation which ordinarily induces highly localized damaged regions in most cases, in the case of granular YBCO, a global improvement in the Tc is therefore expected due to redistribution of evolved oxygens from the ion tracks as observed in our sample.

## VIII.4. Conclusion

Irradiated with 120 MeV S ion (with $S_e < S_{eth}$) induce only point defects in sintered granular YBCO thck films and cause a faster degradation

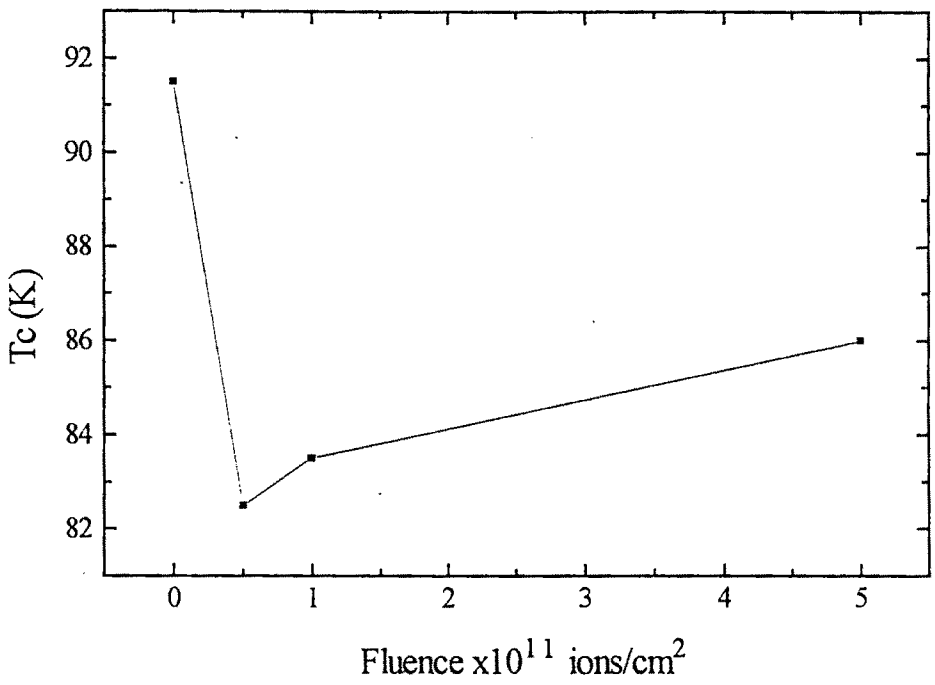


Fig. VIII.6. Variation of Tc with 250 MeV Ag-ion irradiation fluence in YBCO/Ag (10 wt.%) composite thick film. At the first dose of irradiation, Tc shows a sudden decrease and then slightly increases at higher fluences.

of the grain boundaries as compared to the grain. The superconducting phase coherece across the grain boundaris is therefore suppressed and the samples show semiconducting behaviour. In addition to this general kind of irradiation effect in a granular medium, which has also been seen by others, we see a an interesting aspect of irradiation in inducing improvement in the sample quality with improved grain alignment.

In comparison to YBCO, the YBCO/Ag composite thick films have much suppressed weak link resistivity. Response of this system to SHI irradiation is therefore mostly intragranular. The evolution of this system with fluence when irradiated with 250 MeV Ag ions with $S_e > S_{eth}$ , should be governed by the volume fraction of the amorphized latent tracks and Tc suppression should occur only when current percolation is inhibited by these tracks. Against this expectation, we find a Tc suppression by about 10 K even when the volume fraction of the ion tracks is an order of magnitude less than that required to bring about this change. This result points to an enhanced interaction cross section of the SHI in the medium which we explain in terms of frozen point defects created due to SHI induced secondary electrons.

## References


1. A. Iwase, S. Sasaki, T. Iwata and T. Nihira, Phys. Rev. Lett. **58** (1987) 2450.
2. A. Dunlop, D. Lesueur, J. Morillo, J. Dural, R. Spohr and J. Vetter , C.R. Acad. Sci. Paris. **309** (1989) 1277.
3. E. Paumier, A. Audouard, F. Beuneu, Ch. Dufour, J. Dural, J.P. Girard, A. Hairie, M. Levalois, M.N. Metzner and M. Toulemonde, Rad. Eff. Def. Solids **126** (1993) 181.
4. H. Dammak, A. Barbu, A. Dunlop, D. Lesueur and N. Lorenzelli, Philos. Mag. Lett. **67** (1993) 253.
5. U. Tiwari, N. Sen, A.K. Bandyopadhyay, D. Kanjilal, and P. Sen, Europhys. Lett. **25** (1994) 705.

6. M. Toulemonde, S. Bouffard and F. Studer, Nucl. Instrum. Methods B **91** (1994) 108.
7. S. Klaumunzer and G. Schuhmacher, Phys. Rev. Lett. 51 (1983) 1987
8. Ch. Dufour, F. Beuneu, E. Paumier and M. Toulemonde, Europhys. Lett. **45** (1999) 585.
9. A. Meftah, F. Brisard, J.M. Costntini, E. Dooryhee, M. Hage-Ali, M. Hervieu, J.P. Stoquert, F. Studer and M. Toulemonde, Phy. Rev. B **49** (1994) 12457.
10. S. Hemon, V. Chailley, E. Dooryhee, Ch. Dufour, F. Gourbilleau, F. Levesque and E. Paumier, Nucl. Instrum. Methods B **122** (1997) 563.
11. A. Berthelot, S. Hemon, F. Gourbilleau, C. Dufour, E. Dooryhee, E. Paumier, Nucl. Instrum. Methods B **146** (1998) 437.
12. N.C. Mishra, D.Behera, T. Mohanty, D. Mohanta, D. Kanjilal, G.K. Mehta, R. Pinto, Nucl. Instrum. Methods B **156** (1999) 30.
13. D. Kanjilal, Vacuum, **48** (1997) 979.
14. Y. Sudarsan, Amit Rostogi, S.V. Bhatt, A.K. Grover, Y. Yamaguchi, K. Oka, Y. Nishihora, L. Senapati and D. Kanjilal, Appl. Phys. Lett. **71** (1997) 1576.
15. M.A. Kirk, M.C. Frischherz, J.Z. Liu, L.R. Greenwood and H.W. weber, Philos. Mag. Lett. **62** (1990) 41.
16. O. Meyer, T. Kroener, J. Remmel, J. Greek, G. Linker, B. Strehlau and Th. Wolf, Nucl. Instrum. Methods B **65** (1992) 539.
17. I.E. Rehn, Nucl. Instrum. Methods B **64** (1992) 161.
18. R. Rangel, D.H.. Galvan, E. Adem, P. Bartolo-Perez and M.B. Maple, Supercond. Sci. Technol. **11** (1998) 550.
19. Halbritter, J., Dietrich, M. R., Kupfer, H., Runtsch, B. and Wiihl, H. Z.Phys. B-Condensed Matter **71** (1988) 411.
20. A. Diaz, J. Maza and F. Vidal Phys. Rev. B **55** (1997) 1209.
21. E. Babic, M. Prester, D. Babic, P. Nozar, P. Stastny and F.C. Matacotta, Solid State Commun. **80** (1991) 855.

22. F. Rullier-Albenque, A. Legris, S. Bouffard, E. Paumier and P. Lajay, Physica C **175** (1991) 111.

23. Y. Yan and M.A. Kirk, Phys. Rev. B **57** (1998) 6152.

24. A.D. Marwick, L. Civale, L.K. Elbaum, R. Wheeler, J.R. Thompson, T.K. Worthington, M.A. Kirk, Y.R. Sun, H.R. Kerchner and F. Holtzberg, Nucl. Instrum. Methods B **80/81** (1993)1143.

25. T. Mohanty, N.C. Mishra, K. Patnaik, L. Senapati, D. Kanjilal and G.K. Mehta, Vacuum **48** (1997) 973.

26. D. Behera, K. Patnaik and N.C. Mishra, J. Superconductivity **11** (1998) 641.

27. S. Goto and K. Shik, Jpn. J. Appl. Phys. **34** (1995) 4760.

28. D. Kumar, M. Sharon, R. Pinto, P.R. Apte, S.P. Pai, S.C. Purandare, L.C. Gupta and R. Vijayaraghavan, Appl. Phys. Lett. **62** (1993) 3522.

29. B. Canut and S.M.M Rames Radiation Effects and Defects in Solid **145** (1998) 1.

30. S. Furuno, H. Otsu, K. Hojou and K. Izui, Nucl. Instrum. Methods B **107** (1996) 223.

31. A. Iwase, N. Ishikawa, Y. Chimi, K. Tsuru, H. Wakana, O. Michikami,T. Kambara, Nucl. Instrum. Methods B **146** (1998) 557.

32. A. Miotello and R. Kelly, Nucl. Instrum. Methods B **122** (1997) 458.

33. H. Dammak, A. Dunlop, D. Lesueur, Nucl. Instrum. Methods B **107** (1996) 204.

34 F. Seitz and J.S. Koehler, Sold state Phys. **2** (1956) 305.

35. A.E. Volkov and V.A. Borodin, Nucl. Instrum. Meth. B **107**(1996)172.

36. K. Izui, J. Phys. Soc. Japan **20** (1965) 915.

37. T. Zaepfel, S. Hagmann, J. Ullrich, G. Kraft, H. Schmidt-Boecking, Proceeding of the fourth International Conf. on Swift Heavy ions in Matterials (SHIM-98) Germany 1998 Ed. S. Klaumunzer and N. Stolterfoht.

38 J. Provst, C. Simon, M. Hervieu, D. Groult, V. Hardy, F. Studer and M. Toulemonde, MRS Bulletin, December (1995) 22.

39. S.K. Tolpygo , J.Y. Lin, M. Gurvitch, S.Y. Hou and J.M. Phillips, Phys. Rev. B **53** (1996) 12462 ; ibid 12454.

40. G. Linker, J. Greek, T. Kroener, O. Meyer, J. Remmel, R. Smithey, B. Strehlau and X.X. Xi, Nucl. Instrum. Methods B **59/60** (1991) 1458.

41 E.M. Jackson, B.D. Waver, G.P. Summers, P. Shapiro and E.A. Burke Phys. Rev. Lett. **74** (1995) 3033.

42 P. Monod, K. Maki and F.Rullier-Albenque Phys. Rev. Lett. **75** (1995) 3198.

43. R.P. Gupta and M. Gupta, Phys. Rev. B **45** (1992) 9958.

44 O. Mayer, in studies of high Temperature superconductors edited by A.V. Narlikar Nova series, New York 1989 vol.1 p139); O. Meyer, T. Kroener, J. Remmel, J. Greek, G. Linker, B. Strehlau and Th. Wolf Nucl. Instrum. Methods B **65** (1992) 539.